

# COOLING TECHNIQUES

*S.P. Møller*

Institute for Synchrotron Radiation, University of Aarhus, DK — 8000 Aarhus C, Denmark

## Abstract

After an introduction to the general concepts of cooling of charged particle beams, some specific cooling methods are discussed, namely stochastic, electron and laser cooling. The treatment concentrates on the physical ideas of the cooling methods and only very crude derivations of cooling times are given. At the end three other proposed cooling schemes are briefly discussed.

## 1. INTRODUCTION

The subject of the present lecture is cooling of charged particle beams in storage rings. The lecture is intended to be a general introduction to "all" methods of cooling with emphasis on a physical description and understanding. Detailed theoretical derivations can be found in the referenced literature. Concerning the cooling hardware, no details will be given.

The terms *beam temperature* and *beam cooling* have been taken over from kinetic gas theory. As in the case of a gas, the temperature  $T$  is given by the kinetic energy of the ions,

$$\frac{3}{2} kT = \frac{1}{2} m \langle v^2 \rangle, \quad (1)$$

where  $k$  is the Boltzmann constant and  $m$  the particle mass. Traditionally, the average kinetic energy is also called temperature, and a commonly used unit for temperature is eV. The velocity  $v$  entering the right-hand side of Eq. (1) is the rms value of the ion velocities relative to the average ion velocity, which in a storage ring is non-zero. In this way the temperature is a measure of the disordered motion. Very often the ion beam is not isotropic and one has to specify the longitudinal  $T_{\parallel}$  and the transverse temperature  $T_{\perp}$ , defined by Eq. (1) and the longitudinal and transverse velocity components, respectively. Furthermore, the definition of temperature is only meaningful for a system in equilibrium. Cooling is then a reduction of the beam temperature.

In practice, the transverse emittance  $\epsilon$  [1] and the longitudinal momentum spread  $\Delta p/p$  are used as measures of the transverse and longitudinal temperature, respectively, since these quantities are directly extracted from measurements. The temperature is related to these quantities by the following expressions

$$\frac{3}{2} k T_{\perp} = mc^2 \beta^2 \gamma^2 \epsilon \left( \frac{1}{\langle \beta_H \rangle} + \frac{1}{\langle \beta_V \rangle} \right)$$

$$\frac{3}{2} k T_{\parallel} = mc^2 \beta^2 \langle \Delta p/p \rangle^2$$

where  $\beta$  and  $\gamma$  are the relativistic quantities and  $\beta_H$  and  $\beta_V$  the horizontal and vertical betatron amplitude functions.

The cooling process is characterized by two quantities, namely the cooling time and the final temperature. We shall mainly discuss the cooling times, since the final temperature of the cooled beam is usually determined by an equilibrium between the cooling process and various heating processes. This brings us to the next point, namely why do cooling? The answer is to improve the beam quality. Beam quality is here used in the broad sense of lifetime, transverse and longitudinal emittance and intensity. Furthermore, cooling may counteract heating processes, e.g., intrabeam scattering, multiple scattering on residual gas (and internal targets) and slow instabilities. The intensity increase by alternately cooling and injection is called *accumulation* or *stacking*. It is obtained by adding new particles in regions of phase space cleared of previously injected particles by the cooling system.

If a cooling method is going to be useful, the cooling time must be small and the final temperature low. Furthermore, large beam losses due to the cooling and connected processes are clearly not acceptable, since cooling aims at increasing the particle density.

The Liouville theorem [1] states that for a **continuous fluid** under the influence of **conservative forces**, the phase space density is invariant. The cooling methods circumvent the Liouville theorem in two different ways. The stochastic cooling relies on the fact that a beam of charged particles is not a continuous fluid but consists of many point-like particles. By detection of the phase-space coordinates of samples consisting of a finite number of particles and subsequent correction, the beam can be cooled using conservative forces. Electron cooling, on the other hand, cools the beam with non-conservative forces stemming from collisions between the beam particles and an electron beam.

Synchrotron radiation cooling, or radiation damping, has already been treated in this school by R. Walker [2]. Here we only remind the reader that radiation damping is a very efficient cooling mechanism for electron and positron beams functioning without any cooling hardware. Although synchrotron radiation has been observed from protons in e.g., the CERN SPS, the cooling times for protons are very long, even at the next generation of accelerators, LHC and SSC, to have much significance.

We begin by discussing stochastic cooling and electron cooling in Sections 2 and 3, respectively. These cooling methods have already been shown to be valuable tools in storage rings. The next cooling method, laser cooling, has been extensively used in traps, to achieve very cold samples of ions or atoms. Laser cooling, presently being investigated on ion beams held in a storage ring, will be discussed in Section 4. In Section 5 some more speculative cooling mechanisms will be discussed, and we will compare the different cooling methods and conclude in Section 6.

## 2. STOCHASTIC COOLING

From the invention of stochastic cooling in 1968 to the pay-off with the discovery of the intermediate vector bosons nearly 15 years passed. The father of stochastic cooling, S. van der Meer, was subsequently awarded the Nobel Prize together with C. Rubbia. One of the reasons for this relatively long ripening period was undoubtedly people's blind belief in Liouville. It is also surprising, at first sight, that one can increase the phase-space density by observing, and correcting, the chance variations in the phase-space coordinates of samples of beam particles.

In the following we shall develop the ideas of stochastic cooling and "derive" an expression for the cooling time. For a more complete and rigorous treatment see Ref. [3], in which an extensive list of references and the history of stochastic cooling is to be found. An introduction to stochastic cooling hardware is given in Ref. [4].

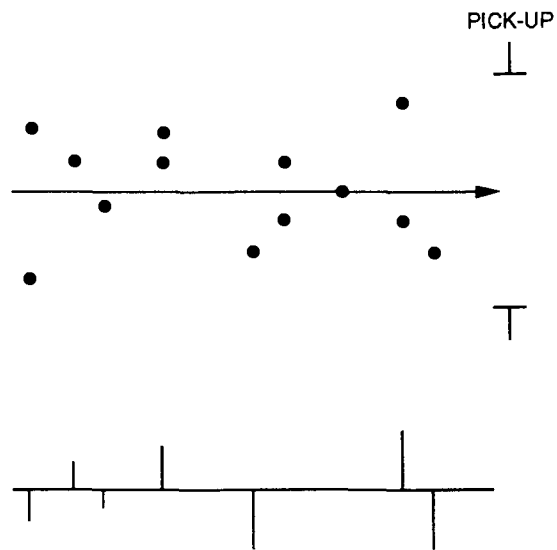


Fig. 1 Ideal signals from a transverse pick-up with infinite bandwidth

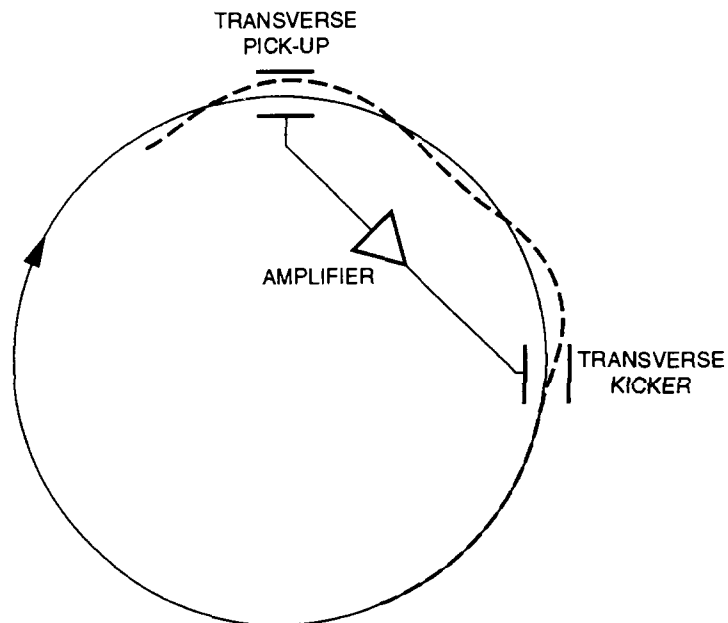


Fig. 2 Principle of transverse stochastic cooling in a storage ring

The particle density along the beam trajectory is a random or "stochastic" quantity for a beam consisting of a finite number of particles. If the beam is observed with a transverse **pick-up**, sensitive to position, the pick-up will give the instantaneous position of the beam centre-of-gravity in the pick-up, Fig. 1. If this sequence of  $\delta$  functions is amplified and applied to a kicker, which re-centers each sample of beam particles, the beam is obviously cooled. If the bandwidth of the pick-up was infinite such that each sample consisted of single particles, and if there was no noise in the system, the beam would have zero emittance after one passage. In reality, the bandwidth is finite and each sample contains many particles. The

situation for transverse stochastic cooling in a storage ring is given in Fig. 2. Because the kicker corrects the angle to the axis, the kicker should be placed an odd number of quarter betatron wavelengths after the pick-up. The situation in Fig. 2 is clearly optimal, since the indicated particle passes the pick-up at the crest of its betatron oscillation. A particle with an additional phase of  $90^\circ$  will not be corrected at all, whereas particles with phases in between will be only partially corrected. Since a storage ring is always designed to have an irrational number of betatron wavelengths per circumference, particles with an unfavourable phase will soon pass the pick-up with a more favourable phase.

Let us now define the term "sample" used above. An off-axis particle passing through a pick-up will give a kicker signal of length  $T_s = 1/2W$ , where  $W$  is the bandwidth of the pick-up-kicker cooling system (Kupfmüller-Nyquist relation). In the same way, a particle passing through the kicker will be influenced by all particles passing the pick-up during a time interval of width  $T_s$ . Consequently, the number of particles in a sample, defined by the smallest fraction of the beam observable by the system, is given by

$$N_s = N/2WT, \quad (2)$$

where  $T$  is the revolution time.

#### Exercise 1.

What is the number of particles per sample in a situation where  $N=10^9$ ,  $W=100$  MHz, and  $T=1 \mu s$  (typical numbers)?

(Central limit theorem). What is the RMS value of the centre-of-gravity of one sample if the sample is rerandomized from passage to passage? Assume a beam with size  $\sigma=5$  mm.

#### Exercise 2 (due to C.S. Taylor).

- 1) Ask for  $N$  random numbers from a normal distribution with zero mean and RMS-value  $\sigma=1$ .
- 2) Find the actual mean value (in general  $\neq 0$ ).
- 3) Subtract error in mean value from each number to restore mean to zero.
- 4) Calculate new  $\sigma'$ .
- 5) Go to step one, replace  $\sigma=1$  with  $\sigma=\sigma'$ , and continue.
- 6) Watch the progress of  $\sigma$ .

Try different values of  $N$ , e.g., 5, 50. The evolution of  $\sigma$  can be very irregular, but in the long term the "beam" is cooled. Use either your pocket calculator or your personal computer. How is the cooling time and the number of particles  $N$  connected?

We are now ready to "derive" the cooling time. Assume that the error at the pick-up of some test particle is  $x$  and the applied correction is  $\lambda x$ . In general,  $\lambda \neq 1$ . The corrected position of the test particle will then be given by

$$x_c = x - \lambda x - \sum_{s'} \lambda x_i, \quad (3)$$

where the last term corresponds to the kicks from the other particles in the sample. The kick from the test particle itself is called the coherent term and the sum of kicks from the other particles in the sample is called the incoherent term. These two terms can be added by including in the sum all particles in the sample

$$x_c = x - \lambda \sum_s x_i . \quad (4)$$

The sum can now be expressed by the average error of the particles in the sample

$$\langle x \rangle_s = \frac{1}{N_s} \sum_s x_i \quad (5)$$

as

$$x_c = x - \lambda N_s \langle x \rangle_s = x - g \langle x \rangle_s , \quad (6)$$

where  $g \equiv \lambda N_s$  is the fractional correction usually called the *gain*. Accepting, intuitively, that it is unhealthy to correct more than the observed error of the sample,  $g \leq 1$ , we assume  $g = 1$ . Let us furthermore neglect the incoherent term in Eq. (3), which should give a best performance estimate. We then get the single passage correction

$$\Delta x = x_c - x = - \frac{1}{N_s} x , \quad (7)$$

giving us the cooling rate per turn

$$\frac{1}{\tau_n} = - \frac{1}{x} \frac{dx}{dn} = - \frac{\Delta x}{x} = \frac{1}{N_s} \text{ per turn} . \quad (8)$$

The cooling rate per second can now be obtained by multiplication of Eq. (8) with the revolution frequency. Substituting Eq. (2) for  $N_s$ , we get

$$\frac{1}{\tau} = \frac{1}{T} \frac{1}{N_s} = \frac{2W}{N} . \quad (9)$$

Surprisingly, this expression only overestimates the optimal cooling time by a factor of 2. (Compare Eq. (9) to the cooling time seen in Exercise 2.)

It is a matter of taste whether one likes the manipulations in the above derivation. Clearly, one has to justify the assumptions. Much more rigorous derivations can be found in Ref. [3] both in time domain and in frequency domain. The general expression for the cooling rate reads

$$\frac{1}{\tau} = \frac{2W}{N} [2g - g^2(M+U)] . \quad (10)$$

The first term is identified as the coherent terms and the second is the incoherent term due to the other particles in the sample ( $M$ ) and due to the noise in the system ( $U$ ). Actually,  $U$  is the noise-to-signal ratio, which increases as the cooling proceeds. The quantity  $M > 1$  is also called the *mixing factor*. The reason why  $M > 1$ , is that there is no complete rerandomization from the kicker to the pick-up. In other words, the samples are not random samples. Actually, there is also a small mixing term, which decreases the coherent term, due to the mixing between the pick-up and the kicker. The mixing is mainly due to the momentum spread in the

beam, and by a clever design of the cooling ring it is possible to minimize the mixing between the pick-up and the kicker while having a strong mixing between the kicker and the pick-up. There are, however, many other restrictions on the lattice. The optimum cooling time is given by

$$\tau = \frac{N}{2W} (M+U) \quad (11)$$

obtained for

$$g = \frac{1}{M+U} . \quad (12)$$

**Exercise 3.**

Verify this (by differentiation)!

From Eqs. (11) and (12) we see that the cooling time increases as the cooling proceeds, due to the increasing influence of the noise. We also see that optimally the gain has to be reduced during the progress of the cooling, but the cooling never stops even for very small signal-to-noise ratios. The cooling time is proportional to the number of stored particles, and stochastic cooling favours low-intensity and hot beams. The last and most important quantity in Eq. (11) is the bandwidth which has to be as large as possible. For the Fermilab antiproton collector and the ACOL at CERN,  $W$  is up to several GHz. For  $W=1$  GHz and the ideal situation  $U=0$  and  $M=1$  we have  $\tau=1s$  for  $N=10^9$ . In practice,  $\tau$  is around an order of magnitude larger.

**Exercise 4.**

Include noise in the computer model from Exercise 2 by adding some random number to the "observed" mean value.

The cooling system described above is directly applicable for horizontal and vertical betatron cooling. Two ways of momentum cooling have been suggested. In both cases the transverse kicker is replaced by a longitudinal acceleration/deceleration gap. In the Palmer method the momentum deviation from the nominal is detected by a transverse pick-up placed in a high dispersion region. Remember  $\Delta x/x = D_x \Delta p/p$ . Inevitably, there will also be an influence from the betatron motion to the detected signal. In the same way, momentum cooling may lead to transverse heating. The other method detects the momentum by sensing the revolution frequency,  $\Delta f/f = \eta \Delta p/p$ . One big advantage of this method is that the pick-up is a sum pick-up, giving a much larger signal than a transverse difference pick-up. This filter method of Thorn-dahl transforms the detected signal to a correction signal by placing a so-called notch filter between the preamplifier and the power amplifier.

Stochastic cooling was first investigated at ISR and ICE at CERN, and is now routinely used at the antiproton rings LEAR, AA, and ACOL at CERN, and the antiproton collector at Fermilab in USA. The cooling times have constantly been decreasing by utilizing pick-up-amplifier-kicker systems of larger and larger bandwidths and less noise. Stochastic momentum cooling has also been tested at TARN in Japan, and stochastic cooling is also going to be used at the heavy-ion storage rings COSY and ESR in Germany.

### 3. ELECTRON COOLING

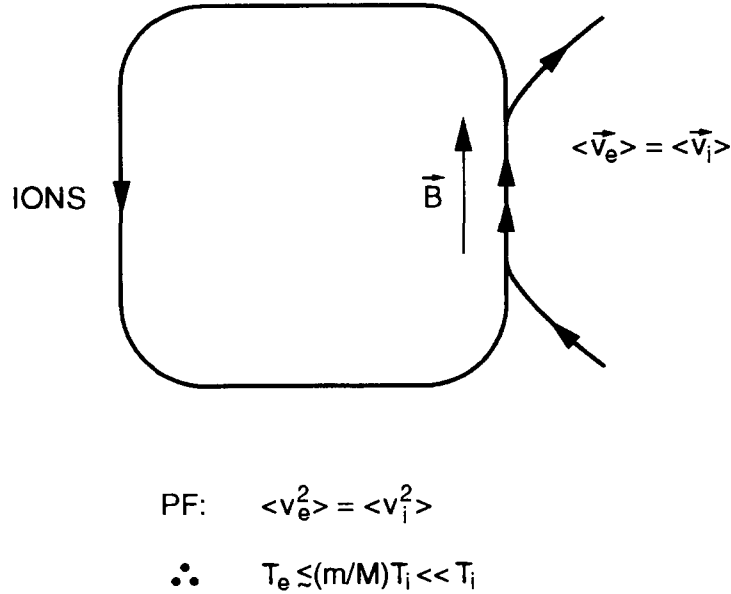


Fig. 3 Principle of electron cooling in a storage ring

Electron cooling was proposed by G. Budker in 1966, and the first electron cooling experiments were performed by his group in Novosibirsk. Electron cooling was subsequently investigated at ICE at CERN and at Fermilab, and very recently at LEAR at CERN. Electron cooling is now the cornerstone of the many low-energy cooler rings, LEAR, IUCF, TSR, CELSIUS, CRYRING, ASTRID, COSY and ESR. For an extensive review of electron cooling, see Ref. [5]. The process of electron cooling can, at least conceptually, be understood with analogy to kinetic gas theory. A stored ion beam is electron cooled by merging the ion beam in a straight section with a cold (monochromatic and parallel) equivelocity electron beam, as sketched in Fig. 3. In the laboratory frame the situation is as in Fig. 4a, but in the so-called particle frame, moving with the average ion velocity, things look different, Fig. 4b. In Fig. 4 the thick arrow represents an ion and the thin arrows correspond to electrons. In this particle frame the situation is analogous to the heat exchange when mixing two gases of different temperatures in a container. By collisions the temperature of the two gases will equalize. Since the electron gas is constantly renewed, the ion temperature will tend towards the electron temperature when neglecting heating processes. In the beginning of the cooling process the ion velocity is typically larger than the electron velocity (averages in the particle frame)

$$\langle v_I^2 \rangle \geq \langle v_e^2 \rangle \quad (13)$$

implying that initially

$$T_I^i \equiv \frac{1}{2} M \langle v_I^2 \rangle \gg \frac{1}{2} m \langle v_e^2 \rangle \equiv T_e^i, \quad (14)$$

since we only consider the electron cooling of heavy particles. In equilibrium

$$T_I^f = T_e^f \quad (15)$$

and

$$v_I^{\text{rms}} \equiv \sqrt{\langle v_I^2 \rangle} = \sqrt{\frac{m}{M}} v_e^{\text{rms}} \sim \frac{1}{43} \sqrt{\frac{1}{A}} v_e^{\text{rms}}, \quad (16)$$

so finally the velocity spread of the ions will be much smaller than the velocity spread of the electrons. The cooling process can also be considered as the slowing down of the ions in the electron gas in analogy with the usual stopping of charged particles in matter.

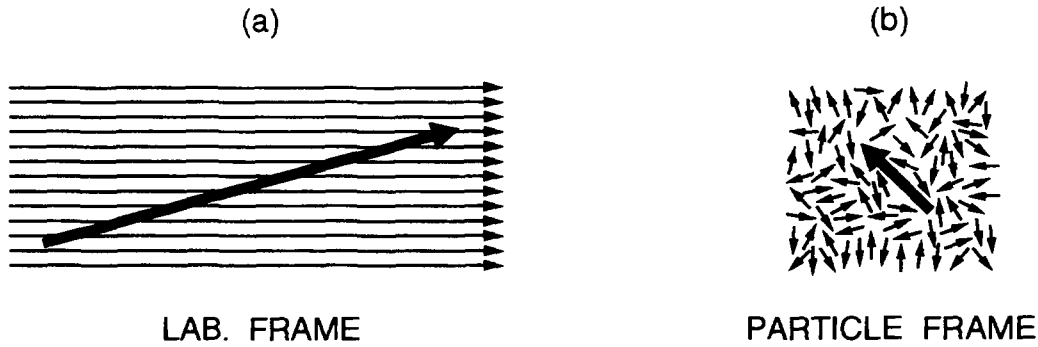


Fig. 4 Electron cooling in the laboratory frame and in the particle frame

We shall now obtain the cooling time by deriving an expression for the drag (or frictional) force in the binary encounter model, where the ion-electron beam interaction is treated as a series of independent two-particle collisions. Although the electron beam in practice (see later) is moving in a longitudinal magnetic field  $B$ , we will first assume  $B=0$ . The influence of the magnetic field on the cooling time will be discussed later. We consider binary collisions, where an ion of velocity  $v_I$  collides with an electron of velocity  $v_e$ . In the rest frame of the ion, Fig. 5, the electron of velocity  $w = v_e - v_I$  is scattered by the much heavier ion through an angle  $\theta$  acquiring a velocity  $w'$ , where  $w' = w$ . In a time  $dt$ , the average momentum transfer to the ion is

$$-dp = (dnw dt) \sigma(\theta, w) d\Omega m(w' - w), \quad (17)$$

where  $\sigma(\theta, w)$  is the differential scattering cross section,  $d\Omega$  the solid angle around  $\theta$  into which the electrons of mass  $m$  are scattered, and  $dn = nf(v_e) d^3v_e$  the density of electrons with velocity within  $d^3v_e$ . Here  $n$  is the homogeneous spatial electron density and  $f(v_e)$  the velocity distribution. The cooling force is now obtained from Eq. (17) by integration over scattering angle and relative velocity

$$F = mn \int d^3v_e f(v_e) w \sigma_{tr}(w) w \quad (18)$$

where the so-called transport cross section is given by



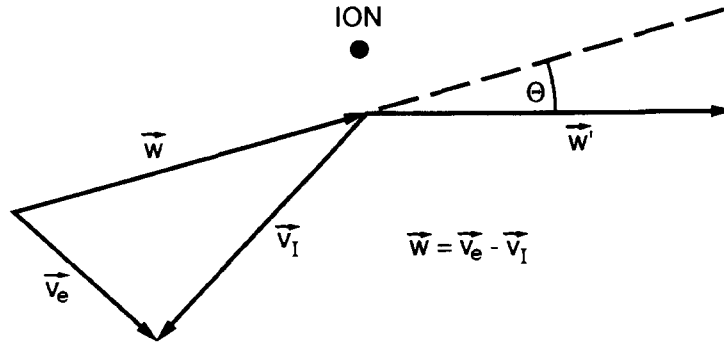


Fig. 5 Binary collision in particle frame

$$\sigma_{tr}(w) = \int_0^{\pi} (1 - \cos \theta) \sigma(\theta, w) 2\pi \sin \theta d\theta . \quad (19)$$

The differential cross section for collisions between two point-like particles, neglecting spin, is the Rutherford cross section  $\sigma \propto \sin^{-4} \theta/2$ . As is well-known from stopping theory, this cross section leads to a logarithmic divergence of the transport cross section at small angles. In practice, this divergence is avoided by introduction of a non-zero minimum scattering angle,  $\theta_{\min}$ . The physical justification for this cut-off is that for small scattering angles, corresponding to large impact parameters, the process is not a two-body scattering, and the other electrons screen the ion-electron interaction potential at large distances. If we denote the screening length  $\lambda$ , the cut-off is given by

$$\theta_{\min} = d/\lambda, \quad d = 2 |Z| e^2 / m w^2 , \quad (20)$$

where  $Ze$  is the projectile charge. We are now able to write the friction force as

$$\mathbf{F} = Z^2 \frac{2\pi n e^4}{m} \int d^3 \mathbf{v}_e L f(\mathbf{v}_e) \frac{\mathbf{w}}{w^3} , \quad L = \log(2\lambda/d) , \quad (21)$$

where  $L$  is known as the Coulomb logarithm. The cooling time, characteristic of the cooling process, may be determined from the relation

$$\tau^{-1} \equiv \left| \frac{1}{v_I} \frac{dv_I}{dt} \right| = \left| \frac{F}{M v_I} \right| . \quad (22)$$

To obtain the cooling time in the laboratory frame, one has to multiply the cooling time in the particle frame with  $\gamma^2$  stemming from the time dilation and the Lorentz contraction of the electron beam. The cooling time may be obtained in the limits of high ( $v_I > v_e^{\text{rms}}$ ) and low ( $v_I < v_e^{\text{rms}}$ ) ion velocities. For high ion velocities the electron velocity may be replaced by a

$\delta$  function, i.e., stationary electrons. For low ion velocities we use an isotropic Maxwell distribution

$$f(v_e) = \frac{e^{-v_e^2/\langle v_e^2 \rangle}}{\pi\sqrt{\pi}\langle v_e^2 \rangle^{3/2}}, \quad T_e = \frac{1}{2} m \langle v_e^2 \rangle. \quad (23)$$

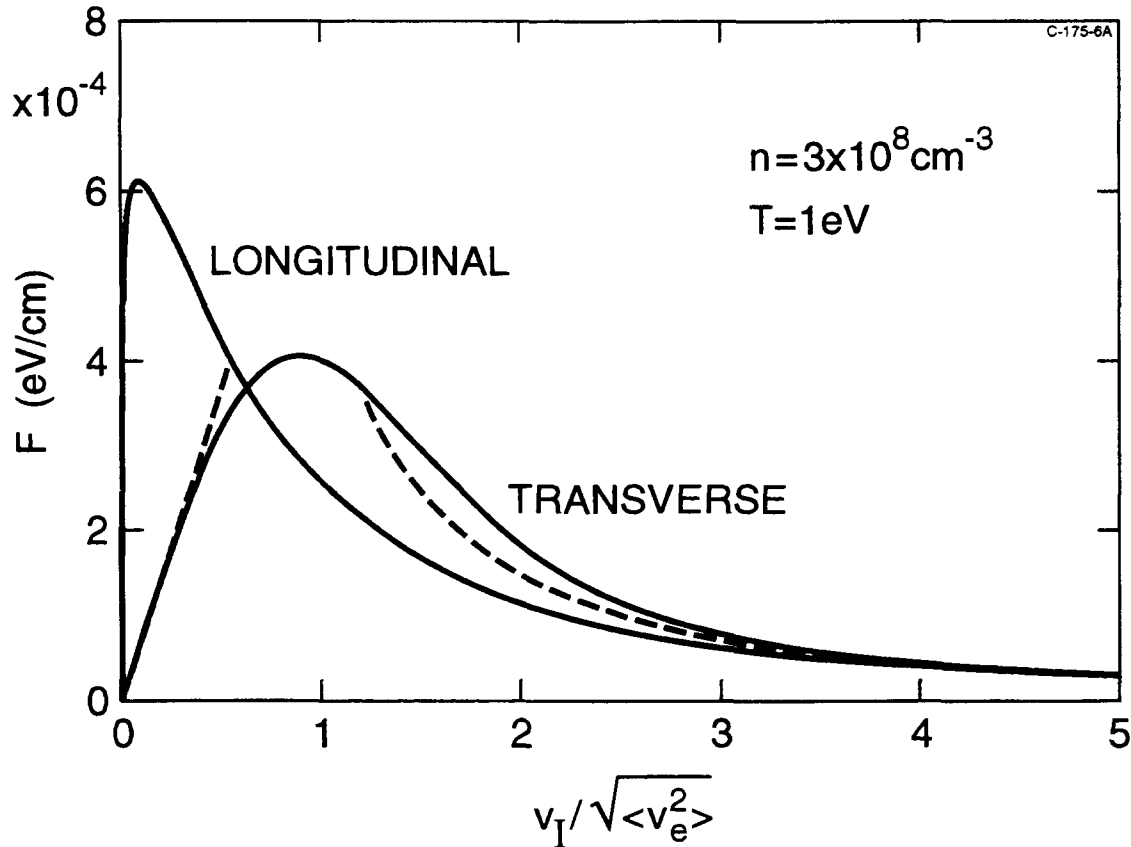


Fig. 6 Drag force on a proton in a flattened electron gas as function of projectile velocity. The dashed curves give the asymptotic behaviours derived in the text.

The result for the cooling time in the two limits is

$$\tau = \frac{\gamma^2}{\eta} \frac{Mm}{Z^2 e^4} \frac{1}{n_L L} \begin{cases} \frac{1}{4\pi} v_I^3 & v_I > v_e^{\text{rms}} \\ \frac{3}{2\sqrt{2\pi}} \left( \frac{T_e}{m} \right)^{3/2} & v_I < v_e^{\text{rms}} \end{cases}, \quad (24)$$

where  $\eta$  is the ratio of the length of the cooling section due to the ring circumference and  $n_L$  the laboratory electron density. This expression deserves several comments. First of all, cooling becomes unfavourable for ultra-relativistic energies,  $\gamma \gg 1$ . The cooling time is small for light ions of high charge state. Furthermore, the cooling section should be long and the

electron beam dense. The cooling time of hot beams is proportional to  $v_I^3$ , disfavouring very hot beams. The cooling of cold ion beams is independent of the ion temperature and proportional to  $T_e^{3/2}$ . The two limits of the cooling force are drawn in Fig. 6 as dashed lines. In a typical case ( $T_e=0.2$  eV,  $v_I < v_e$ ,  $n_L=3 \cdot 10^8 \text{ cm}^{-3}$ ,  $L=10$ ,  $\eta=0.05$ ,  $\gamma=1$ ,  $Z=1$ ) we get a cooling time of 40 s.

Next, we discuss two important modifications to the above treatment. In reality, the electron velocity distribution is not Maxwellian. Due to the acceleration of the electrons in the

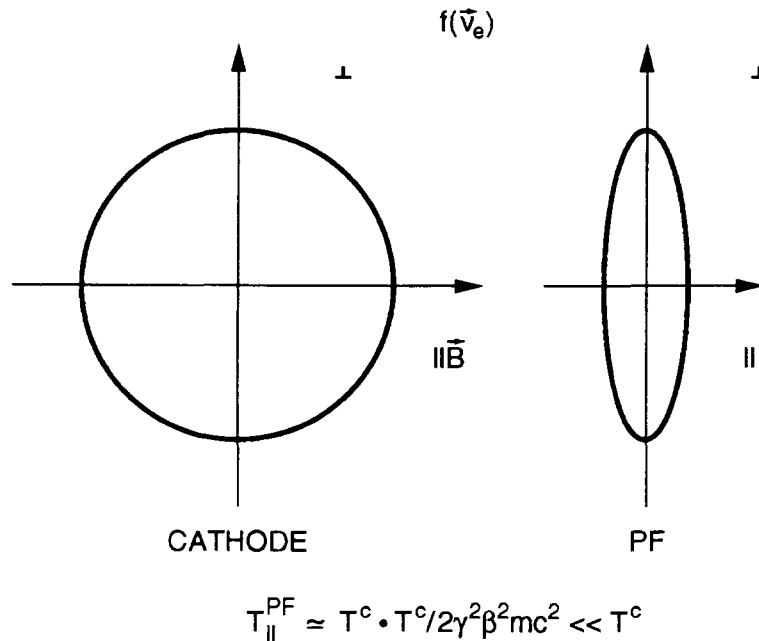


Fig. 7 The electron velocity distribution at the cathode and after the acceleration, where it is flattened.

electron gun, the velocity distribution becomes flattened in the longitudinal direction, Fig. 7. The longitudinal temperature in the particle frame is given by

$$T_{\parallel}^{PF} = T_c^2 / 2\gamma^2 \beta^2 mc^2 \ll T_c, \quad (25)$$

**Exercise 5.**

Derive eq. (25).

where  $T_c$  is the cathode temperature. The transverse temperature is unchanged. This longitudinal velocity compression clearly extends the high ion velocity regime in the above calculation for the longitudinal cooling to much smaller ion velocities, leading to much shorter longitudinal cooling times for low longitudinal ion temperatures. Also the transverse cooling time is reduced somewhat due to this flattening. In Fig. 6 (from Ref. [7]) is shown a computation of the drag force for protons in a flattened electron gas as a function of projectile velocity. The drag force is shown for a pure longitudinal and a pure transverse ion velocity.

The other assumption in the above derivation, which does not correspond to reality, is concerned with the magnetic field  $B$ . In actual setups a longitudinal magnetic field guides and confines the electron beam throughout the interaction region. In this magnetic field the

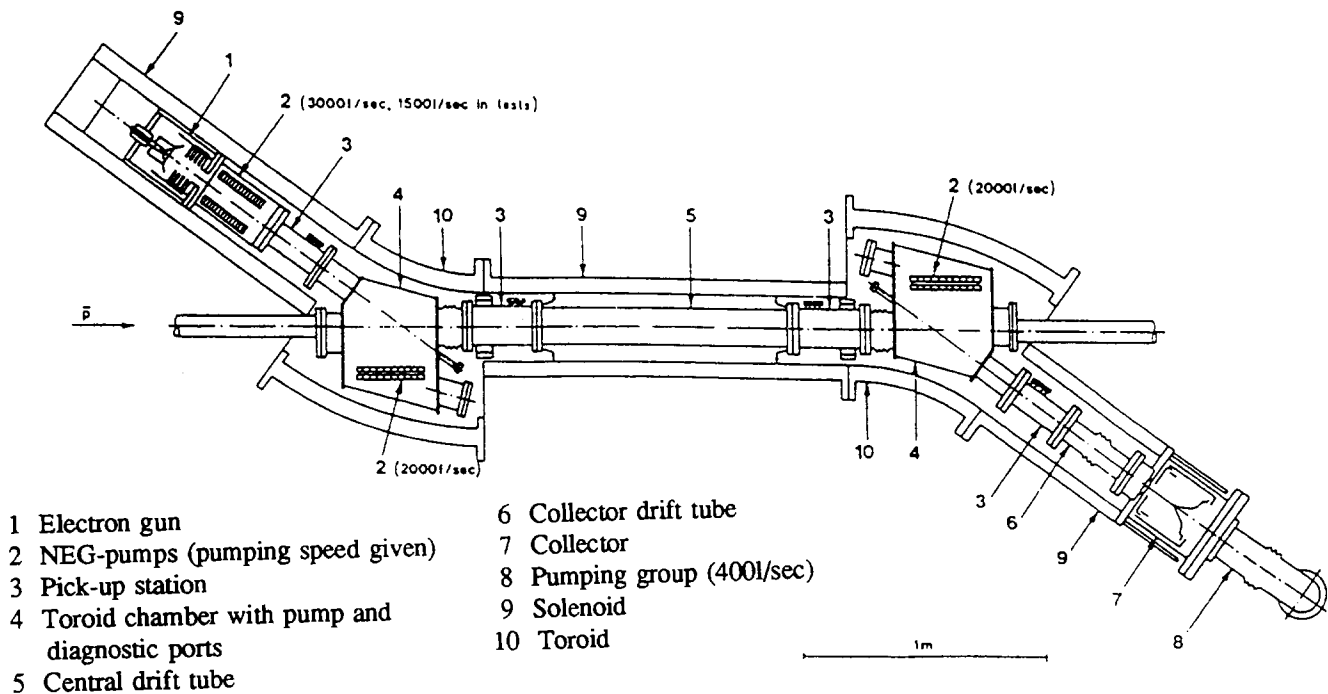


Fig. 8 LEAR electron cooler

electrons will perform a cyclotron motion, superimposed on their longitudinal drift, with revolution frequency given by the cyclotron frequency  $\omega_c = eB/mc$ . An analytic binary collision treatment is only possible for infinitely strong magnetic fields, in which case the electrons appear to be of zero transverse temperature. In general, if  $1/\omega_c$  is small compared to the collision time, the influence of the transverse motion averages out. The inclusion of a strong longitudinal magnetic field leads to very short cooling times for transverse cooling. The combination of a flattened electron distribution and a strong longitudinal magnetic field is usually referred to as *super cooling*, and cooling times less than one tenth of a second are in principle obtainable.

Several problems arise in the binary encounter approximation outlined above. A complementary calculation [6], treating the electron beam as a continuous fluid, avoids these problems. Such a description is clearly expected to be good for the distant collisions, where problems with screening and other collective phenomena arise in the binary approximation. In this calculation the drag force can also be calculated for finite magnetic fields. We shall not discuss this model further, but refer to Ref. [7], where the binary and the dielectric descriptions are combined to give fairly easy-to-evaluate expressions for the drag force.

The typical electron cooler assembly is basically the same as shown in Fig 8. The electron source is normally a thermo-cathode. The cathode is surrounded by a Pierce shield giving a parallel electron beam. The cathode is at the high negative potential and the electrons are accelerated through the anodes to ground potential, where they enter the drift region. The electrons are magnetically confined in a solenoidal field. A section of a toroid bends the

electrons into the interaction region, also contained in a solenoid. Another toroid section bends the electrons into the collector section, where they are decelerated before being dumped. The efficiency of the collector is very important due to the high power in the electron beam, typically amperes up to 100 kV. Loss of electrons furthermore gives rise to a high gas load. Large outgassing is a severe problem at both the cathode and the collector end, since many coolers aim at a pressure in the  $10^{-11}$ - $10^{-12}$  torr region. Therefore, many pumps with large pumping speeds are installed in electron coolers.

The electrons leave the cathode with a temperature of a few tenths of an eV. To preserve this low temperature, the magnetic guide field has to be very homogeneous. Also the high-voltage supply has to be highly stabilized. Also worth mentioning is the non-negligible radial space-charge potential in an intense electron beam and the influence of the cooler magnetic fields on the ion beam, which also has to be considered. Finally, the equivelocity electron beam will also lead to loss of ions owing to recombination. The rate is, however, several orders of magnitude smaller than the cooling rate, but in the case of singly-charged particles the neutral atoms formed are very useful to diagnose the cooling process.

#### 4. LASER COOLING

Laser cooling of atoms and ions in electromagnetic traps is today a well-known and widely used technique. It was suggested in Ref. [8] also to use laser cooling for ions in a storage ring.

The idea is basically the following: Ions with some electrons attached have a discrete absorption spectrum. When using this frequency selectivity in connection with the Doppler shift in frequency, ions with different velocities can be distinguished. The Doppler-shifted frequency of the laser photons seen by an ion in the beam is

$$\omega' = \gamma\omega(1 - \beta\cos\theta) , \quad (26)$$

where  $\beta$  and  $\gamma$  are the usual relativistic factors and  $\theta$  the angle between the ion velocity and the incident laser pulse. Ions that have a velocity  $\beta$  so that  $\omega' = \omega_{AB}$ , corresponding to a transition  $A \rightarrow B$ , may absorb photons, which are subsequently reemitted. Since the photon absorption is unidirectional, whereas the radiation emission is isotropic, the ions will on the average have their velocity changed (momentum conservation). Here we shall only discuss longitudinal cooling, in which case the laser beam is merged with the ion beam in a straight section of a storage ring. Transverse cooling may (at least in principle) be performed having another laser beam at some angle to the ion beam at the expense of a small overlap. For simplicity, we consider ions with only two energy levels A and B, so that the ions can be excited from A to B and decay from B to A. The cooling process is sketched in Fig. 9. In one absorption-emission process the ion acquires on the average the recoil velocity

$$v_r = \hbar q/M = \hbar\omega_{AB}/Mc , \quad (27)$$

where  $\hbar q$  is the photon momentum and  $M$  the ion mass. Clearly, photons carry little momentum and a large number of photons must be scattered by each ion to make a significant change of the ion momentum. The number of photon absorptions and emissions depend on the number of photons in the laser beam and the lifetime of state B. When the photon intensity is too large, however, stimulated emission becomes dominant, and no cooling is performed since the emitted photons are then coherent with the laser photons. Hence, a short cooling time requires

a short decay time of the upper level. The development of the ion-velocity distribution during the cooling process is shown in Fig. 10. Two lasers, which have a frequency width much smaller than the Doppler width of the beam, are used; one (Laser #1) copropagating and one

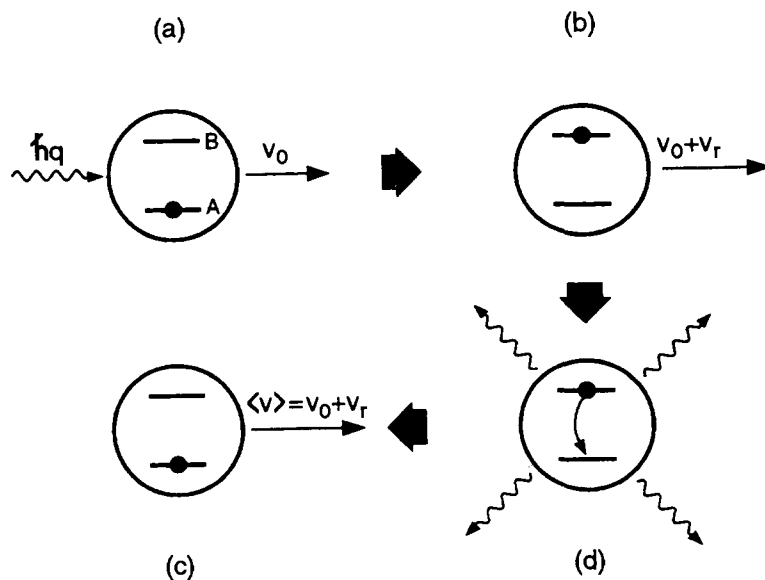


Fig. 9 Photon absorption-emission cycle responsible for laser cooling

(Laser #2) counterpropagating with the beam. Ions in resonance with a laser will be accelerated (Laser #1) or decelerated (Laser #2). Laser #1 scans the Doppler profile during the process of cooling. Ions, which are in resonance with the laser, recoil to higher velocities, and when the laser has crossed the Doppler profile, the ion beam is confined longitudinally between the lasers. Laser #1 merely act as a snow plough, pushing the ions ahead of it.

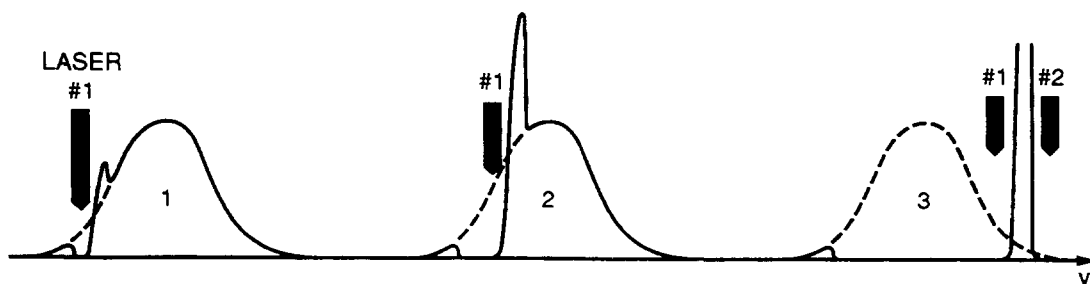


Fig. 10 Change in ion-velocity distribution caused by the laser during the laser-cooling process

As an example, let us consider the case of a 100-keV  ${}^7\text{Li}^+$  beam. The ion has a closed transition from the metastable  ${}^3\text{S}(1s2s)$  to the  ${}^3\text{P}(1s2p)$  of  $5485\text{\AA}$ , which can be reached by CW dye lasers. The lifetime of the upper state is 43 ns. The change in energy of an ion from one photon absorption-emission corresponds to  $\Delta E=12$  meV. If we choose a laser power so that the stimulated emission rate equals the spontaneous emission, we have a spontaneous rate of  $1.2\cdot 10^7/\text{s}$ . This corresponds to a few mW in a beam spot of 5 mm, which is a moderate power density. Then, we have approximately 15 photon absorption emission cycles in an interaction region of 2m, corresponding to a change in energy of 0.2 eV. An ion beam from a well-stabilized separator has an energy spread of one eV, so the cooling time will correspond to a few revolution times, typically a few tenths of  $\mu\text{s}$ . The ultimate temperature corresponds to a single recoil kick of 12 meV.

We have seen above that laser cooling has the potential of a very fast cooling process, and that very low temperatures can, in principle, be reached. The main problem with laser cooling is that it is not universal. Few ion species with appropriate energy-level schemes exist that can be reached by tunable lasers. The only (?) known species are  ${}^7\text{Li}^+$  ( $1s2s$ ),  ${}^9\text{Be}^+$ ,  ${}^{24}\text{Mg}^+$ , and  ${}^{166}\text{Er}^+$ .

Laser cooling has recently been demonstrated at TSR and ASTRID on  ${}^7\text{Li}^+$  [9],  ${}^9\text{Be}^+$  and  ${}^{166}\text{Er}^+$ . Momentum spreads of less than  $10^{-6}$  have been obtained for dilute  $\text{Li}^+$  beams. Also transverse cooling is being investigated.

## 5. OTHER COOLING METHODS

Several other cooling methods have been proposed, but the question is whether these cooling methods are useful, because — although the beam is cooled — an appreciable fraction of the beam may be lost due to competing processes. More than 20 years ago Kolomensky suggested the so-called **ionization cooling** [10]. The method is equivalent to electron cooling but the electron beam is replaced by a foil. The problem is clearly that ions are lost or acquire very large momentum changes due to electron capture and large-angle scattering on nuclei. Kilian has proposed a **radiative cooling of ions** [11]. The idea is that intrabeam scattering [12] excites ions, which subsequently de-excite radiatively. In this way, internal energy in the circulating beam is emitted as photons, and the relative motion of the ions is damped. A strong bunching is needed to provide sufficient collision energy to excite ions. On the other hand, charge-changing collisions should be avoided. The principle of this cooling method is very attractive, since the beam is cooled in all directions, since no cooling hardware is needed and since it gets better the denser the beam is. However, the method still has to be demonstrated both theoretically and experimentally. Finally we mention **dielectronic cooling**, which was recently proposed by Schuch [13]. Dielectronic recombination is the process of electron capture, where the energy gained in the capture process is spent to excite another electron. The final state is thus a doubly excited ion with a charge one unit higher than the original one. If the ion auto-ionizes before the first magnetic element, on the average the ion has gained the momentum of the captured electron, since the electron emission process is isotropic. The process is a kind of resonant electron scattering, similar to the 'resonant photon scattering' in laser cooling. Also the feasibility of this cooling method has to be proven. Other cooling methods can still be invented, but they will probably not be as universal as stochastic and electron cooling.

## 6. CONCLUSION AND COMPARISONS

In the table below, stochastic, electron, synchrotron radiation, and laser cooling are compared. The characterizations are clearly crude, but the differences between the methods are easily seen. Stochastic cooling and electron cooling are rather universal, whereas laser and synchrotron radiation cooling works only for some special ions and electrons/positrons, respectively. To some extent, the two first mentioned cooling methods are also complementary. Stochastic cooling works best for hot beams whereas electron cooling times get shorter the colder the beam. This has led sceptics to say that stochastic cooling gets worse and worse as the cooling process proceeds, whereas electron cooling only works when it is not needed. The truth is probably that a combination of the two cooling methods is ideal. The stochastic cooling system collects the tails of the beam and the electron cooling system freezes the core of the beam. The choice between electron and stochastic cooling is also influenced by the velocity regime. Stochastic cooling favours high velocities, whereas electron cooling becomes technologically demanding for relativistic beams.

Radiation damping and, in the last few years, stochastic cooling and electron cooling have already proved their usefulness for storage rings. Recently, laser cooling has been demonstrated on  ${}^7\text{Li}^+$ ,  ${}^9\text{Be}^+$  and  ${}^{166}\text{Er}^+$ . Momentum spreads of less than  $10^{-6}$  have been obtained for dilute  $\text{Li}^+$  beams, and perhaps laser-cooled beams will enter a new regime of low temperatures.

**Table 1**  
Comparison of cooling methods

	Stochastic	Electron	Synchrotron radiation	Laser
Species	all	ions	$e^+/e^-$	some ions
Favoured beam velocity	high	medium $0.01 \leq \beta \leq 0.01$	very high $\gamma \geq 100$	any (but Doppler)
Beam intensity	low	any	any	any
Cooling time	$N \cdot 10^{-8} \text{ s}$	$1 \cdot 10^{-2} \text{ s}$	$\sim 10^{-3} \text{ s}$	$\sim 10^{-4} - 10^{-5} \text{ s}$
Favoured beam temperature	high	low	any	low



## REFERENCES

- [1] A.H. Sørensen, 3rd General Accelerator Physics Course, Proc. 1988 CERN Accelerator School, Ed. S. Turner, CERN 89-05 (1989) 18, and J. Buon, 4th General Accelerator Physics Course, Proc. 1990 CERN Accelerator School, Ed. S. Turner, CERN 91-04 (1991) 30.
- [2] R. Walker, Present proceedings.
- [3] D. Möhl, Advanced Accelerator Physics Course, Proc. 1985 CERN Accelerator School, Ed. S. Turner, CERN 87-03 (1986) 453 ff.
- [4] C.S. Taylor, Antiprotons for Colliding Beam Facilities, Proc. 1983 CERN Accelerator School, CERN 84-15 (1984) 163 ff.
- [5] J. Bossert, 4th Advanced Accelerator Physics Course, Proc. 1991 CERN Accelerator School, Ed. S. Turner, CERN 92-01 (1992) 147.
- [6] A.H. Sørensen and E. Bonderup, Nucl. Instrum. Methods 215 (1983) 27.
- [7] A.H. Sørensen, ECOL 1984, Ed. H. Poth, Karlsruhe, Germany.
- [8] P.J. Channell, J. Appl. Phys. 52 (1981) 3791.
- [9] S. Schröder et al., Phys. Rev. Lett. **64** (1990) 2901.  
J.S. Hangst et al., Phys. Rev. Lett. **67** (1991) 1238.
- [10] A.N. Skrinsky and V.V. Parkhomchuk, Sov. J. Part. Nucl. 12 (1981) 223.
- [11] K. Kilian, CERN EP 84-05, unpublished.
- [12] A.H. Sørensen, General Accelerator Physics Course, Proc. 1986 CERN Accelerator School, Ed. S. Turner, CERN 87-10 (1987) 135 ff.
- [13] R. Schuch, Symp. Ion Cooler Ring Experiments, Abisko, Sweden, May 4-5, 1988, unpublished.